Ovalbumin(323−339) Peptide Binds to the Major Histocompatibility Complex Class II I-A^d Protein Using Two Functionally Distinct Registers†

Benjamin J. McFarland,‡ Andrea J. Sant,§ Terry P. Lybrand,‡,|| and Craig Beeson*,‡

Departments of Chemistry and Bioengineering, University of Washington, Seattle, Washington 98195, and Department of Pathology, University of Chicago, Chicago, Illinois 60637

Received June 17, 1999; Revised Manuscript Received October 5, 1999

ABSTRACT: Proteins of the class II major histocompatibility complex (MHC) bind antigenic peptides that are subsequently presented to T cells. Previous studies have shown that most of the residues required for binding of the chicken ovalbumin (Ova) 323−339 peptide to the I-A^d MHC class II protein are contained within the shorter 325−336 peptide. This observation is somewhat inconsistent with the X-ray structure of the Ova peptide covalently attached to I-A^d (1IAO structure) in which residues 323 and 324 form binding interactions with the protein. A second register for the Ova(325−336) peptide is proposed where residues 326 and 327 occupy positions similar to residues 323 and 324 in the 1IAO structure. Two Ova peptides that minimally encompass the 1IAO and alternate registers, Ova(323−335) and Ova(325−336), respectively, were found to dissociate from I-A^d with distinct kinetics. The dissociation rates for both peptides were enhanced when the His81 residue of the MHC β-chain was replaced with an asparagine. In the 1IAO structure the βH81 residue forms a hydrogen bond to the backbone carbonyl of I323. If the Ova(325−336) peptide were also bound in the 1IAO register, there would be no comparable hydrogen-bond acceptor for the βH81 side chain that could explain this peptide's sensitivity to the βH81 replacement. The Ova(323−335) peptide that binds in the 1IAO register does not stimulate a T-cell hybridoma that is stimulated by Ova(325−336) bound in the alternate register. These results demonstrate that a single peptide can bind to an MHC peptide in alternate registers producing distinct T-cell responses.

A key regulatory step in the generation of an immune response is the activation of helper T cells by peptides bound to MHC[1] class II proteins. The MHC class II proteins are highly polymorphic $\alpha\beta$-heterodimers expressed on the surface of specialized antigen-presenting cells. Crystallographic analyses (*1*−*9*) have shown that the peptide is bound to the membrane distal surface of the protein in a groove formed by two helices atop a β-sheet platform (Figure 1, top). The bound peptide is in an extended conformation similar to a polyproline II helix with most of its backbone hydrogen-bonded to conserved MHC residues (*4*). Peptide side chains directed into the binding groove reside in "pockets" delineated by most of the polymorphic residues. In most of the MHC class II proteins there are four major pockets, designated P1, P4, P6, and P9, where the numbering refers to the peptide side chain residing in the pocket (Figure 1, bottom). Most of the remaining peptide side chains are directed out of the MHC peptide binding pocket where they can interact with the T-cell receptor (TCR).

Because MHC class II proteins must present a wide variety of antigenic peptides, they have evolved promiscuous peptide-binding sites. Sequencing of peptides eluted from cellular MHC proteins has revealed a diverse collection of peptides with ragged N- and C-termini that extend out of the open ends of the binding groove (*10*−*12*). In one sense, the presence of the array of hydrogen bonds to the peptide backbone constrains the diversity of peptides that can be bound. Only those peptides that can adopt the hydrogen-bond-stabilized backbone conformation without deleterious steric contacts in the binding groove are likely to form stable complexes. In another sense, the presence of the hydrogen bond array allows for promiscuous binding. Any peptide that can adopt the required backbone conformation can presumably form stable complexes without high complementarity between "anchoring" side chains and the MHC pockets. Indeed, in the recently reported crystal structures of two peptides bound to the murine MHC class II protein I-A^d, little complementarity between peptide side chains and the MHC pockets is observed (*9*). It seems reasonable then to suggest that some peptides might bind to the MHC protein in alternate registers that differ only in the relative location of peptide side chains within the MHC pockets.

Several observations have suggested heterogeneity in the binding of a single peptide to an MHC class II protein. Although the dissociation of peptides from the MHC proteins is typically monophasic, several peptides have been identified that dissociate from their restricted MHC protein with biphasic dissociation kinetics (*13*−*21*). In some of these cases

† This work was supported by NSF Grant MCB-9722374 (C.B.) and NIH Grant R01 AI34359 (A.J.S.) and NIH grant P01DK 49841 (T.P.L.). B.J.M. was supported by NIH National Research Service Award 5 T32 GM08268 from the National Institute of General Medical Sciences.

* Corresponding author: Phone 206-616-8493; E-mail beeson@chem.washington.edu.

‡ Department of Chemistry, University of Washington.

§ University of Chicago.

|| Department of Bioengineering, University of Washington.

[1] Abbreviations: MHC, major histocompatibility complex; TCR, T-cell receptor; IEF, isoelectric focusing; k_{app}, apparent first-order dissociation rate constant; wt, wild-type.

10.1021/bi991393l CCC: $18.00
Published on Web 11/24/1999

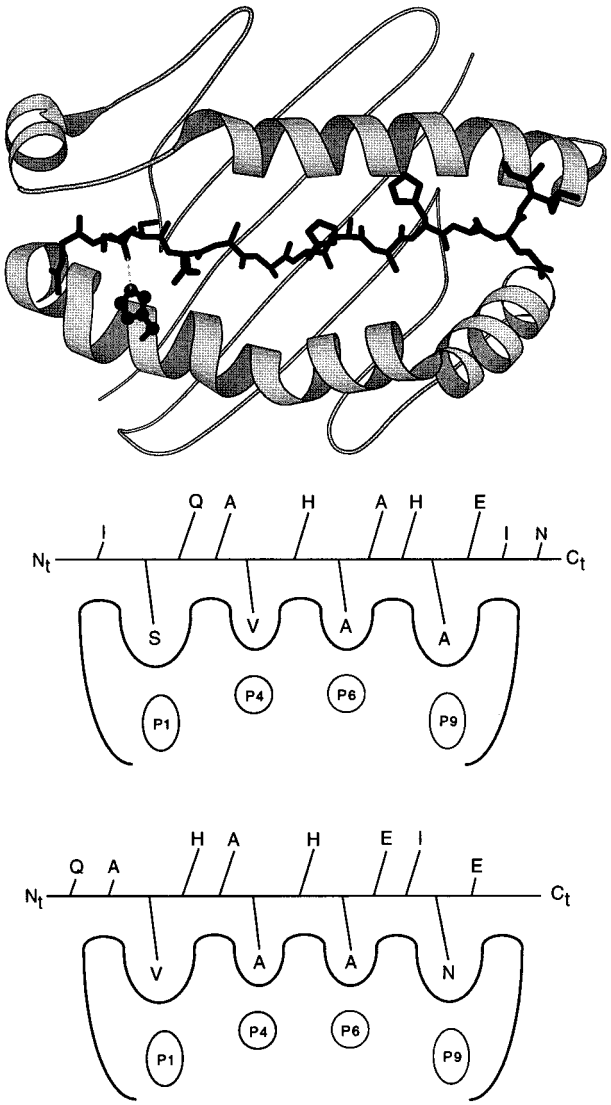

FIGURE 1: Structures of the Ova peptide bound to the MHC class II protein I-A^d. (Top) Shown is a ribbon diagram of the Ova(323−339) complex generated from the coordinates of the 1IAO crystal structure (9). The perspective is of the membrane apical face of the protein showing the peptide-binding groove formed by the α-helix (top) and β-helix (bottom) above a β-sheet platform. The Ig domains are not shown for clarity. The peptide lies within the groove in a polyproline II-like conformation with the its N-terminus to the left of the illustration. Also shown is the βH81 side chain in a ball-and-stick representation at the bottom left. (Bottom) Shown are schematics of the Ova peptide bound to I-A^d in two different registers. The register observed in the 1IAO crystal structure is illustrated on the top (residues 323−335 are shown). An alternate register, proposed here, is shown in the bottom of the figure (residues 325−336 are shown). In both representations, peptide side chains that occupy the MHC P1, P4, P6, and P9 pockets are directed down into the protein schematic and peptide side chains that are potential TCR contacts are directed upward. Residues of Ova(323−335) and Ova(325−336) that are required for recognition by the 3DO-54.8 and 8DO-51.15 T-cell hybridomas, respectively, are elevated above other potential TCR contacts. The βH81 side chain forms a hydrogen bond to the peptide carbonyl immediately N-terminal to the left of the P1 pocket. The complete sequence for Ova(323−339) is ISQAVHAAHAEINEAGR.

it was shown that the biphasic dissociation arises from a stable intermediate in the dissociation reaction (*15, 19, 20*). In other cases it was suggested that the peptide bound to the MHC in distinct registers or at different sites (*16, 18*). It has also been shown that a single peptide can induce T-cell responses that discriminate between the manner in which the peptide−MHC complex was generated, leading again to the suggestion of isomeric peptide−MHC complexes (*22, 23*). A study of overlapping, cross-reactive peptides that differed in the residues required for MHC binding has led to the proposal that peptides might even bind in a different orientation within the groove (*24*). In support of this suggestion, a recent combined modeling and binding study has provided evidence for a peptide bound to the human DQ0302 MHC protein with its termini in an orientation reversed with respect to the canonical binding mode (*25*).

To eliminate the problems associated with the promiscuous binding of MHC proteins, a strategy for linking the peptide to the N-terminus of the β-chain with a flexible (Gly Ser)$_n$ linker was developed (*26*). This strategy was used to generate a complex of the Ova(323−339) peptide bound to I-A^d for crystallographic analysis (*9, 27*). Even though the recombinant Ova−I-A^d complex was homogeneous with respect to composition, subsequent preparative isoelectric focusing (IEF) separation gave several isoforms (*27*). It was shown that these isoforms did not differ in glycosylation and it was concluded that some of the isoforms could be due to different registers for the bound peptide. One of the isoforms of the Ova(323−339) peptide covalently linked to I-A^d gave crystals of sufficient quality for crystallographic analysis. The solved structure, 1IAO, shows the peptide bound in a canonical conformation with little complementarity between MHC pockets and the enclosed peptide side chains (*9*). Previous studies have shown that most of the residues required for stable binding of Ova(323−339) to I-A^d are contained within the shorter 325−336 peptide (*28*). This observation is somewhat inconsistent with the 1IAO crystal structure, in which the side chain of Ser324, not contained within Ova(325−336), is seen to occupy the P1 pocket. However, the shorter peptide in the 1IAO register could bind with measurable affinity because of the array of backbone hydrogen bonds near the peptide's C-terminus. An alternative explanation for the apparent discrepancy between binding studies and the 1IAO crystal structure is that the Ova(323−339) peptide binds in alternate registers as suggested by the IEF analysis of the covalent Ova−I-A^d construct (*27*). We had previously proposed a register for the Ova peptide bound to I-A^d that differs from that observed in the crystal structure, herein referred to as the alternate register (*17*). In the alternate register, the valine side chain observed to be in the P4 pocket of the crystal structure was proposed to reside instead in the P1 pocket (Figure 1, bottom). The alternate register was proposed on the basis of binding studies (*28*) and molecular modeling (*17*). We provide evidence here demonstrating that the Ova(323−339) can indeed bind to I-A^d using distinct registers.

EXPERIMENTAL PROCEDURES

Peptide Synthesis. Peptides were synthesized with standard Fast-MOC chemistry on an Applied Biosystems 431A peptide synthesizer and labeled on the N-terminus with the *N*-hydroxysuccinimidyl ester of 5(6)-carboxyfluorescein before cleavage. Cleavage from the resin was achieved with 92.5% trifluoracetic acid, 5% water, and 2.5% thioanisole, and crude peptides were then purified by reverse-phase HPLC (acetonitrile/water gradient with 0.1% TFA). Identity of the purified peptides was confirmed by electrospray mass

spectrometry, and concentrations of peptide solutions were obtained through absorbance measurements of the fluorescein label in bicarbonate buffer (pH 8.9) at 495 nm.

Dissociation Rates of Peptide−MHC Complexes. I-A^d protein was isolated as described previously (*16*, *17*). In brief, L-cells expressing I-A^d were lysed and passed over a lentil lectin column that was subsequently eluted with methyl mannoside onto an affinity column (MK-D6 antibody). The protein was eluted from the antibody column with Na_2CO_3 (pH 11.5) and dialyzed into phosphate-buffered saline with 0.2 mM dodecyl maltoside. Purity of the protein was assessed with silver-stained SDS−PAGE, and concentrations were determined with a Micro BCA assay. To measure the rate of dissociation of fluorescein-labeled peptides, a solution of I-A^d protein and a 30−50-fold excess of peptide was incubated at pH 5.3 at 37 °C for 18 h. Unbound peptide was then removed by size exclusion (Sephadex G50-SF) at 4 °C and pH 7.4. The reaction mixture was separated by high-performance size exclusion chromatography using a 30 cm by 7.5 mm TSK3000SW column (Toso Haas, Montgomeryville, PA) and a fluorescence detector. At the beginning of the dissociation, the initial amount of labeled peptide bound to the MHC was measured as the peak height of the peptide/MHC fraction. After subsequent incubations at 37 °C, the relative peak height at each time was used as a measure of peptide still bound to the protein. Apparent first-order dissociation rate constants (k_{app}) were obtained from single-exponential fits to the monophasic dissociation data. Dissociation data that are apparently biphasic were fit with double-exponential functions and both the component pre-exponential terms and exponential constants (k) are reported.

T-Cell Stimulation. T-cell responses to antigen were assessed by measuring the amount of IL-2 present in culture supernatants after incubation of 1×10^4 T cell hybridomas with 1×10^4 A20 cells and 10 μg/mL peptide. Incubations were carried out in triplicate for 48 h in 96-well flat-bottom plates in a total volume of 200 μL of growth medium containing RPMI 1640 supplemented with 10% fetal calf serum. Supernatant (50 μL/well) was transferred to another 96-well plate and frozen at −80 °C. Relative amounts of IL-2 in the supernatants were determined by adding IL-2-dependent HT-2 indicator cells (1×10^4/well) and measuring proliferation of the cells after 24 h by an MTT assay.

Molecular Modeling Studies. All models for the Ova-I-A^d peptide complex were based on the recent 1IAO crystal structure (*9*). Models with single point mutations in either MHC (e.g., βH81N in the β-chain) or peptide were generated with the interactive graphics modeling package PSSHOW (*29*). The alternate register model was generated by use of a standard polyproline type II helix backbone conformation from the 1IAO crystal structure. The PSSHOW program was used to replace all side chains with the appropriate residues for the alternate register sequence. Standard side-chain conformations were selected from a rotamer library. All models were refined with limited energy minimization (100−200 cycles), followed by low-temperature molecular dynamics for 1−2 ps at 20 K. All molecular mechanics calculations were performed in vacuo with a distance-dependent dielectric constant, using a standard all-atom potential function (*30*). After initial model refinement, molecular dynamics simulations were performed for all MHC−peptide complexes for 5−10 ps at both low temperature (20 K) and room temperature (298 K) to examine the nature and stability of peptide−MHC contacts. The AMBER suite of programs was used for all molecular mechanics calculations (*31*), and the final model structures were analyzed with PSSHOW and MD-DISPLAY (*32*).

RESULTS

Native Peptides Exhibit Complex Dissociation Kinetics. Because of the kinetic complexity of binding reactions between peptides and MHC protein (*33*), we chose to use the more readily interpreted peptide dissociation rates as a measure of relative binding capacity of different Ova peptides for I-A^d. The dissociation of Ova(323−339) from I-A^d is complex, however, giving rise to a kinetic curve that is at least biphasic (Figure 2A). About 20% of the Ova(323−339) peptide−MHC complexes dissociate with an apparent rate constant of approximately $(2.1 \pm 0.8) \times 10^{-4}$ s^{-1} (Table 1). The remaining peptide−MHC complexes are very long-lived, dissociating with an apparent rate constant of $(3.5 \pm 0.3) \times 10^{-6}$ s^{-1}. The longer Ova(323−339) peptide was truncated to identify shorter core peptides that minimally encompass the 1IAO crystal structure and alternate registers, respectively. The first peptide evaluated was Ova(323−335), which includes all of the residues observed in the 1IAO crystal structure. Dissociation of this peptide from I-A^d was at least biphasic (Figure 2B), similar to that seen for the full-length peptide. An even shorter peptide, Ova(323−333), that only occupies positions P(−1) to P10 in the 1IAO structure also exhibits biphasic dissociation kinetics (not shown).

The Ova(325−336) peptide that minimally encompasses the alternate register exhibits monophasic kinetics in its dissociation from I-A^d (Figure 2C). The stability of the alternate register Ova(325−336) peptide [$k_{app} = (2.6 \pm 0.3) \times 10^{-6}$ s^{-1}] is comparable to that of the long-lived complexes observed in the dissociation kinetics for the full-length Ova(323−339) and shorter Ova(323−335) peptides. The peptide Ova(326−336) that further eliminates binding contacts observed in the 1IAO structure also binds stably to I-A^d [$k_{app} = (8.0 \pm 0.4) \times 10^{-6}$ s^{-1}]. The peptide Ova(325−333) that encompasses the overlapping sequences of the two minimal core peptides does not form long-lived complexes with I-A^d (data not shown). Thus, the peptides that constitute the core of the 1IAO and alternate registers, Ova(323−335) and Ova(325−336), respectively, exhibit distinct dissociation kinetics.

A Model of the Alternate Register Suggests a Variation in Hydrogen Bonding. A model of the Ova(325−336) peptide bound to I-A^d in the alternate register was derived from the 1IAO crystal structure. Visual inspection of this model after limited energy minimization suggested that the alternate register is chemically and physically plausible. The anchor residues in pockets P1 (valine), P4 (alanine), P6 (alanine), and P9 (asparagine) exhibit good steric and chemical complementarity with the anchor pockets. This model maintains the polyproline type II helix backbone conformation observed in the 1IAO (*9*) and other MHC class II crystal structure complexes (*1*−*8*). In fact, the only marked difference in the two registers after energy minimization is the set of probable TCR contacts (see Figure 1). Molecular dynamics relaxation of the 1IAO and alternate register complexes revealed some notable differences, however. In the 1IAO complex, the MHC βH81 side chain forms a hydrogen bond to a backbone carbonyl oxygen of the I323

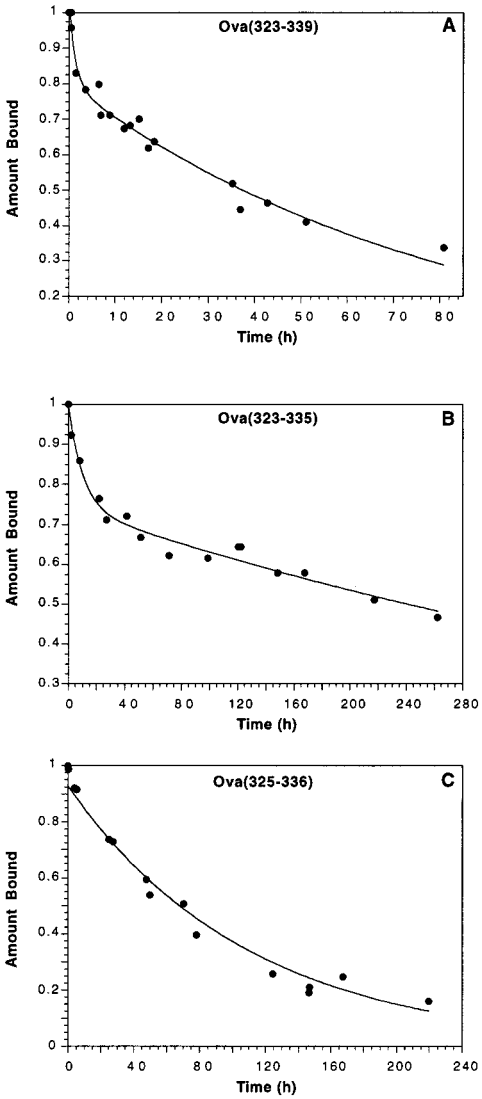

FIGURE 2: Dissociation of Ova(323−339) and two truncated Ova peptides from I-A^d. (A) Dissociation of the full-length Ova(323−339) peptide is at least biphasic. (B) Dissociation of the C-terminal truncated Ova(323−335) is also biphasic. (C) Dissociation of the N-terminal truncated Ova(325−336) is monophasic [$k_{app} = (2.6 \pm 0.3) \times 10^{-6}$ s^{-1}]. MHC protein was incubated with excess fluorescein-labeled peptides for 18 h, excess free peptide was removed by rapid size exclusion, and the amount of fluorescence associated with protein was periodically measured by high-performance size-exclusion chromatography with a fluorescence detector. The fluorescence at each time point (amount bound) was normalized to that measured immediately upon isolation of the peptide−MHC complex. The curves shown in panels A and B are double-exponential functions fit to the data (see Table 1); the curve in panel C is a single-exponential fit to the data. The data in panels A−C each represent compilations of three to four independent dissociation reactions.

peptide residue at the P(−1) position (Figure 1). A similar hydrogen bond between βH81 and the A326 carbonyl was also formed in the alternate register model. After limited dynamics simulation of the 1IAO complex, this hydrogen bond broke quickly and βH81 formed a new hydrogen bond with the carbonyl of the Q325 side chain at the P2 position of the peptide (Figure 3). Only a small rotation of both βH81 and Q325 side chains is required to form the new hydrogen bond. During the course of a 5−10 ps simulation at 298 K, the βH81 side chain alternately hydrogen-bonded with the backbone carbonyl oxygen or Q325 side chain, fluctuating between the two hydrogen-bond partners several times. In the alternate register complex, a histidine side chain (H328) is present at the P2 position, and βH81 cannot reorient to form an alternate hydrogen-bond contact with the H328 side chain, so the original hydrogen bond to the backbone carbonyl oxygen is maintained.

Table 1: Peptide Dissociation Rate Constants[a]

Ova peptide	rate constants ($k \times 10^6$, s^{-1}) wt I-A^d		rate constants ($k \times 10^6$, s^{-1}) H81N I-A^d	
323−339	b[b]	210 ± 80 (0.2)[c] 3.5 ± 0.3 (0.8)		n.d.
323−335	b	27 ± 5 (0.2) 6.1 ± 0.1 (0.8)	m	5.8 ± 0.2
323−335, Q325A	m	2.3 ± 0.3	m	20 ± 0.6
325−336	m	2.6 ± 0.3	m	390 ± 30
325−336, H328Q	b	40 ± 10 (0.7) 15 ± 4 (0.3)	m	2000 ± 200
326−336	m	8.0 ± 0.4	m	370 ± 10

[a] Apparent first-order rate constants were determined from single-exponential fits to monophasic dissociation data. The component rates for biphasic dissociations were obtained from double-exponential fits. [b] Biphasic (b) or monophasic (m). [c] The pre-exponential term from the double-exponential fit.

To test whether the hydrogen-bond fluctuations observed in the 1IAO simulations might be a modeling artifact, we used the modeling results to design additional experiments. The models suggested that replacement of Q325 in the 1IAO structure with alternate residues such as alanine would alter the hydrogen-bonding pattern for the βH81 residue. It was found that an Ova(323−335) peptide in which the Q325 side chain was mutated to an alanine (Q325A) dissociates from I-A^d with monophasic kinetics characterized by a $k_{app} = (2.3 \pm 0.3) \times 10^{-6}$ s^{-1} (Figure 4A). The reversion of Q325A to monophasic dissociation kinetics confirms that the Q325A side chain is involved in MHC binding despite its location outside of the peptide binding groove. The H328 residue occupies the P2 position in the alternate register. It was found that Ova(325−336) peptide in which the H328 side chain was mutated to glutamine (H328Q) dissociates from I-A^d with biphasic kinetics (Figure 4B).

Previous studies have shown that an I-A^d molecule in which the βH81 residue has been mutated to asparagine (βH81N) does not acquire peptides during expression and has reduced capacity for peptide binding (*34*). Presumably the inability of βH81N to form stable peptide−MHC complexes is due to a loss of hydrogen bonding between the βH81 side chain and peptide backbone (*34*). We have shown that the dissociation rates for peptides are enhanced by 20−200-fold for βH81N compared to the native protein (*35*). Models were also generated for a H81N mutant in the I-A^d β chain. The refined 1IAO model and subsequent limited molecular dynamics simulations suggest that the asparagine side chain can alternately form a hydrogen bond with either the P(−1) I323 backbone carbonyl or the P2 Q325 side-chain carbonyl. However, the hydrogen bonds are not predicted to be particularly good, as the geometries are not optimal and the βN81 must adopt a strained (i.e., high-energy) side-chain conformation to interact with the backbone carbonyl or Q325. The modeling results suggested that the dissociation of Ova peptides bound to I-A^d in the 1IAO register would be enhanced for the H81N mutant. It was found that Ova(323−335), the peptide that minimally

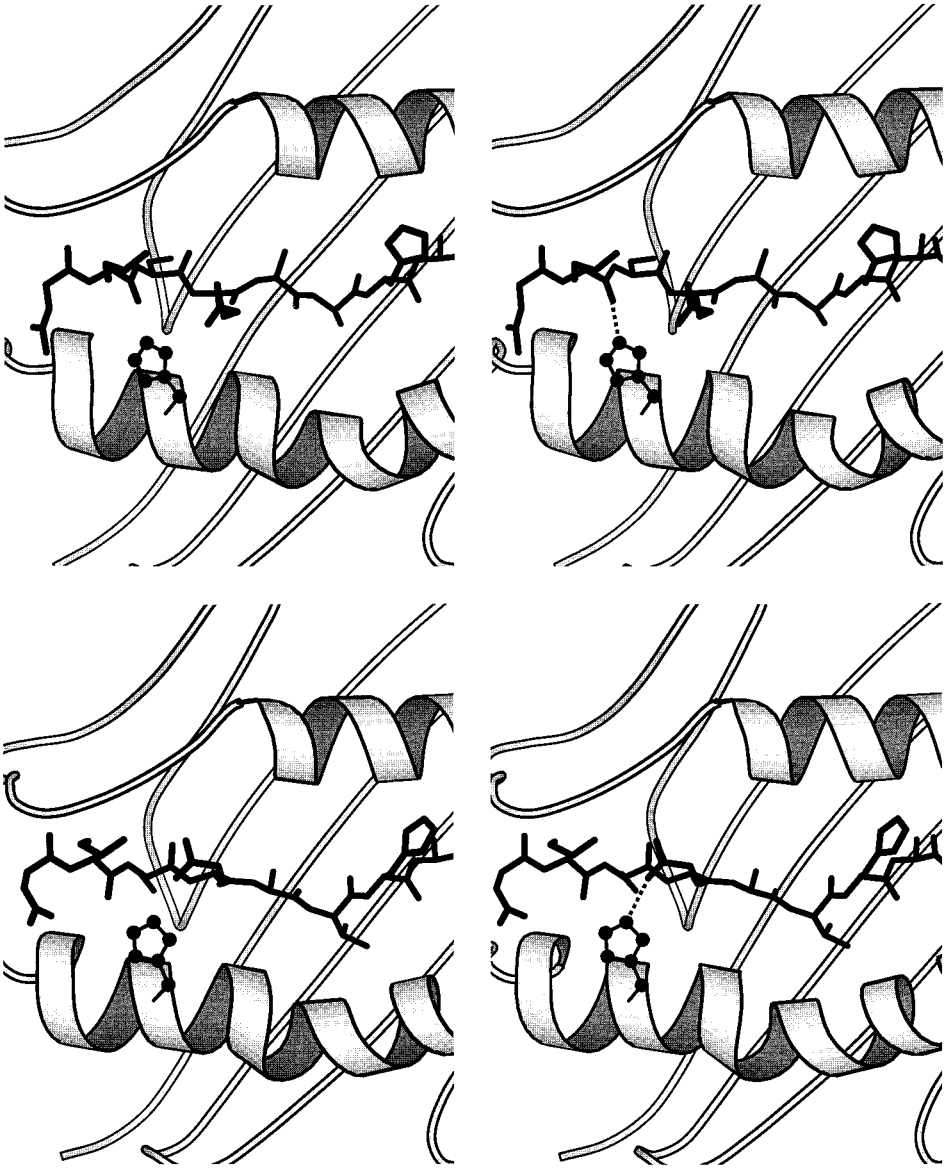

FIGURE 3: Computer models of the 1IAO structure suggest that the βH81 residue can also hydrogen-bond to the side-chain carbonyl of Q325. Shown (top) is a stereoview of the βH81 side chain hydrogen-bonded to the P(−1) carbonyl. Shown (bottom) is a stereoview of a molecular dynamics snapshot in which the βH81 side chain has slightly rotated from the conformer observed in the 1IAO structure to form a hydrogen bond to the Q325 side-chain carbonyl that is directed out of the peptide-binding groove. The conformer shown arises within about 1 ps of a limited molecular dynamics simulation (20 K), suggesting that both rotamer conformers are highly populated. The Q325 residue is at the P2 position in the 1IAO structure (see Figure 1).

encompasses the 1IAO register, dissociates much more rapidly from the βH81N I-A^d protein with $k_{app} = (5.8 \pm 0.6) \times 10^{-6}$ s^{-1} (Figure 4C). The fact that the dissociation kinetics are monophasic further demonstrates the role of the βH81 hydrogen bond in the biphasic dissociations observed for native I-A^d. It was also found that the dissociation rate for the Ova(325−336) peptide from the βH81N I-A^d protein is considerably enhanced relative to that from the wild-type (wt) I-A^d (Table 1).

T-Cell Stimulation Can Discriminate between the Two Binding Registers. T-cell hybridomas generated from mice immunized with whole Ova protein were initially used to identify the Ova(323−339) epitope. The specificity of one of these hybridomas, 3DO-54.8 (*36*), for truncated Ova peptides was evaluated. It was found that the 3DO-54.8 T-cell hybridoma is stimulated by the Ova(325−336) peptide that minimally encompasses the alternate register when presented by antigen-presenting cells expressing I-A^d (Figure 5). Even though the Ova(323−335) peptide that minimally encompasses the 1IAO register also binds stably to I-A^d, it was unable to stimulate the 3DO-54.8 T-cell hybridomas. Previous studies have shown that residues 336−339 are not involved in recognition by these T cells, demonstrating that the inability of this peptide to stimulate the T cells is not due to the absence of these residues (*28*). The full-length Ova(323−339) peptide did stimulate the T-cell hybridomas to the same extent as observed for Ova(325−336), confirming that the full-length peptide binds to I-A^d in both registers.

DISCUSSION

Two sets of results presented here demonstrate that the Ova(323−335) and (325−336) peptides bind to I-A^d using distinct registers. First, the dissociation kinetics for Ova(323−335), a peptide that presumably binds in the 1IAO register, are biphasic. It was shown that the biphasic kinetics are due to a hydrogen bond between the peptide Q325 and

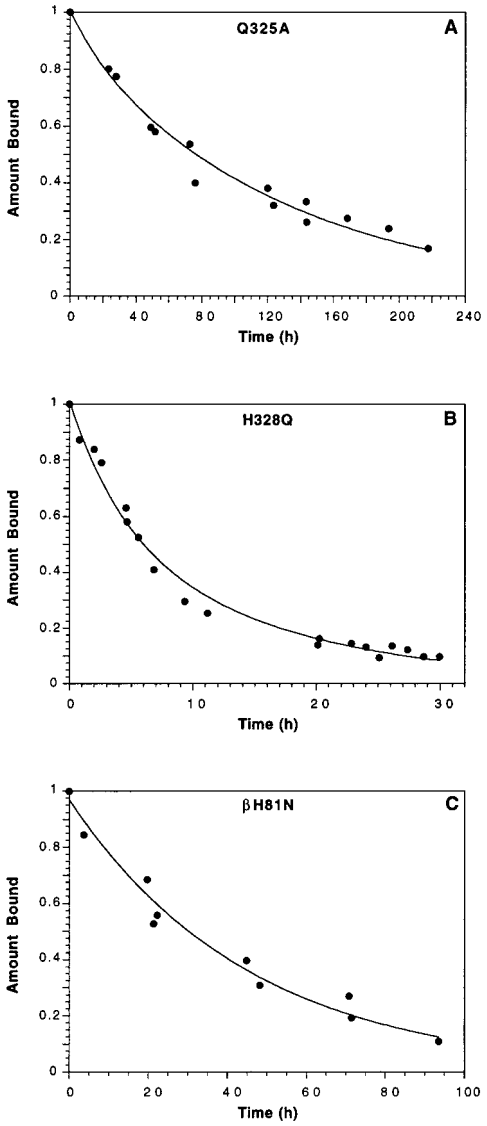

FIGURE 4: Effect of the hydrogen bond between βH81 and Q325 on dissociation kinetics. (A) Dissociation of the Ova(323−335), Q325A peptide−mutant from wt I-A^d is now monophasic [k_{app} = $(2.3 \pm 0.3) \times 10^{-6}$ s^{-1}]. (B) Dissociation of Ova(325−336), H328Q is at least biphasic. The position of H328 in Ova(325−336) is the same as Q325 in Ova(323−335). The data are better fit with a mechanism that includes an intermediate in equilibrium with the fully bound state (not shown). (C) Dissociation of the native Ova-(323−335) peptide from the βH81N I-A^d mutant has also become monophasic [k_{app} = $(5.8 \pm 0.6) \times 10^{-6}$ s^{-1}]. The data in panels A−C are compilations of three to four independent dissociation reactions.

I-A^d βH81 residues. If Ova(325−336) was bound in the 1IAO register, a similar hydrogen bond could be formed. Yet, it was found that the dissociation kinetics for Ova(325−336) are monophasic. Second, the dissociation rate for Ova-(323−335) A325 bound in the 1IAO register was enhanced by mutation of the I-A^d βH81 residue that forms a hydrogen bond to the peptide I323 carbonyl. If the Ova(325−336) peptide was also bound to I-A^d in the 1IAO register, the first peptide residue, Q325, would be in the P2 position (Figure 1). Thus, there would be no carbonyl at the P(−1) position to form a hydrogen bond with the βH81 side chain. In this case it would be predicted that the I-A^d βH81N substitution would have no effect on the dissociation of Ova-(325−336). If, however, the Ova(325−336) peptide was

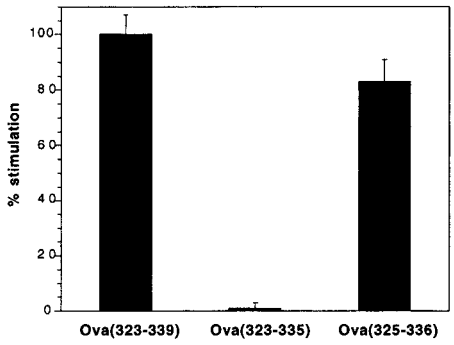

FIGURE 5: The 3DO.54 T-cell hybrid discriminates between Ova-(323−335) and Ova(325−336) bound to I-A^d. Stimulation by each peptide (10 μg/mL) was normalized to the stimulation of the 3DO.54 hybridoma by 10 μg/mL of the full-length Ova(323−339) peptide. Peptides were presented by the A20 B-cell lymphoma and stimulation was assayed as the amount of IL2 released as measured by the proliferation of the IL2-dependent HT-2 cell line.

bound in the alternate register, there would be a backbone carbonyl from A326 at the P(−1) position that could form a hydrogen bond with the βH81 side chain (Figure 1). The observation that the dissociation rate of Ova(325−336) was enhanced by mutation of the I-A^d βH81 residue suggests that the peptide is not bound in the 1IAO register. It could be argued that Ova(325−336) binds in the 1IAO register with a hydrogen bond between βH81 and Q325 that, when disrupted, increases the dissociation rate. However, the dissociation rate of Ova(326−336) is also significantly enhanced for the H81N I-A^d protein.

Numerous studies have suggested that a single peptide can form isomeric complexes with MHC class II proteins that differ in dissociation kinetics (*13*−*21*). In several of these studies it was shown that there is a lag phase in the formation of the long-lived complexes, suggesting that the short-lived complex is a stabilized intermediate in the association and dissociation reactions (*15*, *19*). Presumably these stable intermediates are complexes in which the peptides are partly dissociated from the binding groove. We have shown that the Ova(323−339) and Ova(323−335) peptides dissociate with biphasic kinetics consistent with the formation of a stable intermediate in the dissociation reaction. The observation that these kinetics revert to being monophasic upon mutation of either the peptide Q325 or I-A^d βH81 residues suggests that an interaction between these two residues is involved in formation of the intermediate. As a test for this hypothesis, the H328 residue in Ova(325−336) was mutated to glutamine. It was found that the H328Q peptide dissociated with biphasic dissociation kinetics, an observation that recapitulates the effect of Q325 on the dissociation kinetics for the 1IAO register.

The structure of the intermediate responsible for the biphasic dissociation of the Ova(323−339) peptides is not known. One possibility is that the intermediate is a structure in which the peptide is partly dissociated at the N-terminus but still hydrogen-bonded between Q325 and βH81. Such a hydrogen bond increases the lifetime of the intermediate by slowing either the rate of conversion to the fully bound state and/or the rate for further dissociation. The results observed here suggest that the former is more likely. Disruption of the potential hydrogen bond between Q325 and βH81, achieved through mutation of either residue, eliminates the short-lived phase in the dissociation reactions. If conversion

of the partly dissociated intermediate to the fully bound state is slowed by the formation of a Q325−βH81 hydrogen bond in the intermediate, the probability for a subsequent rapid dissociation would be increased. There is no possibility for a hydrogen bond between βH81 and the P2 side chain in the alternate register [i.e., the Ova(325−336) peptide]. Presumably a partly dissociated species precedes complete dissociation of Ova(325−336), but because of the absence of the stabilizing hydrogen bond, the equilibrium is largely shifted to the fully bound state and only slow, monophasic dissociation kinetics are observed. Substitution of the P2 H328 with a glutamine leads to the formation of rapid, biphasic dissociation kinetics that are apparently caused by a hydrogen bond between the Q328 and βH81 residues. This is supported by the observation that dissociation of the H328Q peptide from the H81N I-A^d mutant is no longer biphasic. The observation that the dissociation rates for the H328Q peptide are increased about 5-fold with respect to Ova(325−336) would suggest that the H328 side chain also forms a binding interaction with the residues on the periphery of the I-A^d peptide-binding groove. The formation of binding interactions between TCR contacts and the MHC protein is relatively common (*37*).

In the absence of a hydrogen bond between βH81 and the P2 side chain [i.e., the Ova(323−335) Q325A and Ova(325−336) peptides] the slow, monophasic dissociation rate is significantly enhanced. However, the two registers differ in their sensitivity to disruption of the hydrogen bond. The dissociation rate for Ova(325−336) is increased about 150-fold while the rate for the Q325A peptide is only increased about 10-fold. These differences in sensitivites are consistent with the assigned binding registers. In both binding registers the most favorable peptide−MHC binding interaction is apparently between the V327 side chain and an MHC pocket. In the 1IAO register the V327 side chain occupies the P4 pocket, but in the alternate register, it occupies the P1 pocket. Since the βH81 residue forms a hydrogen bond to the P(−1) carbonyl directly adjacent to the P1 pocket, it would be anticipated that the Ova(325−336) peptide whose primary V327 residue occupies that pocket would be most sensitive to disruption of the βH81 hydrogen bond.

Several reports have previously suggested that a single peptide can bind to an MHC class II protein in one of several registers. It has been shown that four overlapping peptides derived from sperm whale myoglobin bind to the I-A^d MHC protein producing cross-reactive T-cell responses (*24*). Because the peptide residues required for binding to I-A^d were not strictly shared among the four peptides, it was suggested that the peptides bound in different registers that presented similar antigenic surfaces. Similar results have been reported for the MHC class I protein, a molecule that shares considerable structural homology with the MHC class II proteins (*38*, *39*). However, in all of these studies, peptide−MHC stability was not correlated to the MHC structure, preventing a determination of the binding registers. The fact that the T-cell responses were cross-reactive also leaves some doubt as to the nature of their register in the peptide-binding groove. Here, we have used pairwise mutations of peptide and MHC protein to demonstrate that the Ova(323−339) peptide binds to its restriction element, I-A^d, in two distinct registers that are shifted in register by three residues. Our results are consistent with the observation of multiple isoforms for an I-A^d molecule covalently tethered to the Ova(323−339) peptide (*27*). Our observation that the 3DO 54.8 T-cell hybridoma recognizes only one of the two registers, and the full-length peptide, confirms that both registers are functional and generated during natural antigen processing.

The open ends of the MHC class II binding groove allow for the protein to bind a single peptide in one of several registers. Because peptides eluted from MHC class II proteins are found to have ragged C- and N-termini (*10*−*12*), there is the possibility that they were initially bound in different registers. Numerous studies of naturally processed antigenic peptides have found that T cells responsive to the antigen differ in fine specificities for the peptide residues at the ragged termini outside of the peptide "core" (*40*−*47*). In one of these cases it was shown that T cells discriminated between peptide residues beyond the peptide core because they interacted with CD4, a coreceptor for the MHC class II and TCR proteins (*40*). We suggest that explanation for some of the other reported fine T-cell specificities for residues at the flanking ends of the peptide may be due to the presence of multiple peptide registers as observed here for the naturally processed Ova(323−339) peptide.

ACKNOWLEDGMENT

We thank John Kappler for helpful discussions of unpublished results.

REFERENCES

1. Brown, J. H, Jardetzky, T. S., Gorga, J. C., Stern, L. J., Urban, R. G., Strominger, J. L., and Wiley, D. C. (1993) *Nature (London) 364*, 33−39.
2. Stern, L. J., Brown, J. H., Jardetzky, T. S., Gorga, J. C., Urban, R. G., Strominger, J. L., and Wiley, D. C. (1994) *Nature (London) 368*, 215−221.
3. Ghosh, P., Amaya, M., Mellins, E., and Wiley, D. C. (1995) *Nature (London) 378*, 457−462.
4. Jardetzky, T. S., Brown, J. H., Gorga, J. C., Stern, L. J., Strominger, J. L., and Wiley, D. C. (1996) *Proc. Natl. Acad. Sci. U.S.A. 93*, 734−738.
5. Fremont, D. H., Hendrickson, W. A., Marrack, P., and Kappler, J. (1996) *Science 272*, 1001−1004.
6. Dessen, A., Lawrence, C. M., Cupo, S., Zaller, D. M., and Wiley, D. C. (1997) *Immunity 7*, 473−481.
7. Murthy, V. L., and Stern, L. J. (1997) *Structure 5*, 1385−1396.
8. Fremont, D. H., Monnaie, D., Nelson, C. A., Hendrickson, W. A., and Unanue, E. R. (1998) *Immunity 8*, 305−317.
9. Scott, C. A., Peterson, P. A., Teyton, L., and Wilson, I. A. (1998) *Immunity 8*, 319−329.
10. Rudensky, A. Y., Preston-Hurlburt, P., Hong, S. C., Barlow, A., and Janeway, C. A., (1991) *Nature (London) 353*, 622−627.
11. Hunt, D. F., Henderson, R. A., Shabanowitz, J., Sakaguchi, K., Michel, H., Sevilir, N., Cox, A. L., Appella, and Engelhard, V. H. (1992) *Science 255*, 1261−1266.
12. Vignali, D. A., Urban, R. G., Chicz, R. M., and Strominger, J. L. (1993) *Eur. J. Immunol. 23*, 1602−1607.
13. Sadegh-Nasseri, S., and McConnell, H. M. (1989) *Nature (London) 338*, 274−276.
14. Sadegh-Nasseri, S., Stern, L. J., Wiley, D. C., and Germain, R. N. (1994) *Nature (London) 370*, 647−650.
15. Beeson, C., and McConnell, H. M. (1994) *Proc. Natl. Acad. Sci. U.S.A. 91*, 8842−8845.
16. Witt, S. N., and McConnell, H. M. (1994) *Biochemistry 33*, 1861−1868.
17. Beeson, C., Anderson, T. G., Lee, C., and McConnell, H. M. (1996) *J. Am. Chem. Soc. 118*, 977−980.

18. Tompkin, S. M., Moore, J. C., and Jensen, P. E. (1996) *J. Exp. Med. 183*, 857−866.
19. Rabinowitz, J. D., Liang, M. N., Tate, K., Lee, C., Beeson, C., and McConnell, H. M. (1997) *Proc. Natl. Acad. Sci. U.S.A. 94*, 8702−8707.
20. Schmitt, L., Boniface, J. J., Davis, M. M., and McConnell, H. M. (1998) *Biochemistry 37*, 17371−17380.
21. Schmitt, L., Boniface, J. J., Davis, M. M., and McConnell, H. M. (1999) *J. Mol. Biol. 286*, 207−218.
22. Nelson, C. A., Viner, N. J., and Unanue, E. R. (1996) *Immunol. Rev. 151*, 81−105.
23. Viner, N. J., Nelson, C. A., Deck, B., and Unanue, E. R. (1996) *J. Immunol. 156*, 2365−2368.
24. Nanda, N. K., Arzoo, K. K., Geysen, H. M., Sette, A., and Sercarz, E. E. (1995) *J. Exp. Med. 182*, 531−539.
25. DeWeese, C., Kwok, W. W., Nepom, G. T., and Lybrand, T. P. (1996) *J. Mol. Modeling 2*, 205−216.
26. Kozono, H., White, J., Clements, J., Marrack, P., and Kappler, J. (1994) *Nature (London) 369*, 151−154.
27. Scott, C. A., Garcia, K. C., Stura, E. A., Peterson, P. A., Wilson, I. A., and Teyton, L. (1998) *Protein Sci. 7*, 413−418.
28. Buus, S., Sette, A., Colon, S. M., Jenis, D. M., and Grey, H. M. (1986) *Cell 47*, 1071−1077.
29. Swanson, E. (1995) *PSSHOW*, Seattle, WA.
30. Weiner, S. J., Kollman, P. A., Nguyen, D., and Case, D. A. (1986) *J. Comput. Chem. 7*, 230−252.
31. Pearlman, D. A., Case, D. A., Caldwell, J. C., Seibel, G. L., Singh, U. C., Weiner, P., and Kollman, P. A. (1991) *AMBER*, University of California, San Francisco, CA.
32. Callahan, T. J., Swanson, E., and Lybrand, T. P. (1996) *J. Mol. Graphics 14*, 39−41.
33. Beeson, C., and McConnell, H. M. (1995) *J. Am. Chem. Soc. 117*, 10429−10433.
34. Ceman, S., Wu, S., Jardetzky, T. S., and Sant, A. J. (1998) *J. Exp. Med. 188*, 2139−2150.
35. McFarland, B. J., Beeson, C., and Sant, A. (1999) *J. Immunol. 163*, 3567−3571.
36. Haskins, K., Kubo, R., White, J., Pigeon, M., Kappler, J., and Marrack, P. (1983) *J. Exp. Med. 153*, 1149−1169.
37. Loftus, C., Huseby, E., Gopaul, P., Beeson, C., and Goverman, J. (1999) *J. Immunol. 162*, 6451−6457.
38. Quaratino, S., Thorpe, D. J., Travers, P. J., and Londei, M. (1995) *Proc. Natl. Acad. Sci. U.S.A. 92*, 10398−10402.
39. Owen, J. A., Scinto, L. A., Klein, L., and Kline, C. J., (1986) *Immunology 57*, 499−504.
40. Vignali, D. A., and Strominger, J. L. (1994) *J. Exp. Med. 179*, 1945−1956.
41. Harris, D. P., Vordermeier, H. M., Arya, A., Moreno, C., and Ivanyi, J. (1995) *Immunology 84*, 555−561.
42. Muller, C. P., Ammerlaan, W., Fleckenstein, B., Krauss, S., Kalbacher, H., Schneider, F., Jung, G., and Wiesmuller, K. H. (1996) *Int. Immunol. 8*, 445−456.
43. Nikcevich, K. M., Kopielski, D., and Finnegan, A. (1996) *Cell. Immunol. 172*, 254−261.
44. Quinn, A., and Sercarz, E. E. (1996) *J. Autoimmun. 9*, 365−370.
45. Wilkinson, K. A., Vordermeier, M. H., Kajtar, J., Jurcevic, S., Wilkinson, R., Ivanyi, J., and Hudecz, F. (1997) *Mol. Immunol. 34*, 1237−1246.
46. Huang, C. C., Ts'ao, P. Y., and Manser, T. (1998) *Mol. Immunol. 35*, 279−291.
47. Bartnes, K., Leon, F., Briand, J. P., Travers, P. J., and Hannestad, K. (1999) *Eur. J. Immunol. 29*, 189−195.

BI991393L